

Fraunhofer-Institut für Bauphysik IBP

Forschung, Entwicklung,
Demonstration und Beratung auf
den Gebieten der Bauphysik

Zulassung neuer Baustoffe,
Bauteile und Bauarten

Bauaufsichtlich anerkannte Stelle für
Prüfung, Überwachung und Zertifizierung

Institutsleitung

Univ.-Prof. Dr.-Ing. Gerd Hauser

Univ.-Prof. Dr.-Ing. Klaus Sedlbauer

IBP-Report

Evaluation of the hygrothermal performance of a concrete wall construction with Icynene open cell insulation

Executed on behalf of
Icynene Europe S.P.R.L.

This report contains
9 pages of text
14 figures
1 table

M. Eng. Andrea Binder

Holzkirchen, May 28th, 2014

Abteilungsleiter

Stellv. Abteilungsleiter

Bearbeiter

Dr.-Ing. Hartwig M. Künzel

Dipl.-Ing. Daniel Zirkelbach

M. Eng. Andrea Binder

Content

1	Subject and purpose of examinations	3
2	Design of the study	3
2.1	Design criteria & assessment positions	4
2.2	Construction assembly & materials	5
2.3	Orientation, surface transfer & initial conditions	5
2.4	Boundary conditions	6
3	Results	6
3.1	One-dimensional wall assembly	6
3.2	Two-dimensional joints of wall and ceiling	7
3.2.1	Concrete ceiling	7
3.2.2	Wooden beam ceiling	8
4	Discussion & conclusions	9
5	Figures	10
6	Tables	19

1 Subject and purpose of examinations

Retrofitting exterior walls with insulation affects the constructions' hygrothermal conditions - especially when interior insulation is used. While the effects may be negligible with fewer insulation, they become more pronounced with rising insulation thickness. Lower temperatures inside the wall during winter as well as the rising vapor diffusion resistance towards the interior may lead to increased construction moisture due to a reduced drying potential. In winter, the lower temperatures inside the wall also increase the partial pressure gradient that may rise the moisture content, as humidity from the indoor air enters the construction via vapor diffusion. In some cases, condensation may occur. Convection of humid indoor air through leakages, the absorption of driving rain, and/or construction moisture may also add to these effects. Hence, in order to keep moisture-related harm from the building structure and its inhabitants, (interior) insulation measures need to be carefully planned and evaluated beforehand.

It is the aim of this investigation to evaluate the hygrothermal performance of a hollow-concrete-block wall construction with the climate conditions of Nancy, France, that at its interior side is insulated Icynene open cell spray foam. Here-with, it is of particular interest if the construction shows proper function without the use of an additional vapour retarding layer.

2 Design of the study

The investigations are done with hygrothermal simulation under transient boundary conditions, using the WUFI® software [1]. WUFI® has been developed at the Fraunhofer-Institute for Building Physics (IBP) and has been validated by numerous field and practice tests world wide. It complies with EN 15026 [2] and further international and European standards and guidelines [3, 4, 5] for hygrothermal simulations.

In a first step, the most critical wall orientation needs to be identified, serving as a worst-case scenario for all further simulations. Based hereupon, the one-dimensional performance of a hollow-concrete-block wall without any joints, thermal bridges or else (furthermore called "standard cross section") is analyzed. Practical experience has shown, however, that even when the interior insulation system in itself (i.e. standard cross section) shows proper function, it may well be the joints or thermal bridges of a construction that cause problems. Hence, in a further step, the performance of a thermal bridge is analyzed. For this, the joints of the wall with a concrete ceiling and also with a wooden beam ceiling are analyzed via two-dimensional simulation.

All simulations start at the beginning of the heating period on the first of October and are executed at least until dynamic equilibrium is reached. If not specifically mentioned, all descriptions, results and values in this report refer to floating monthly average values.

2.1 Methodology of assessment & design criteria

All simulations start at the beginning of the heating period on the first of October. For a reliable assessment of the construction, not only the initial behavior during the first years after construction needs to be analyzed, but also the hygrothermal conditions at dynamic equilibrium. Thus, all simulations are executed until any moisture fluctuations are due only to seasonal changes, but no more general accumulation/decrease is shown. In this case, a period of up to 6 years proved to be sufficient.

For the risk assessment, the positions shown in figure 1 and 2 will be evaluated. Hereby, the relative humidity at the surface/interface of the layers will be analyzed. For the standard cross section analyzed with WUFI® Pro, this will be the following positions:

- Rear of insulation (pos. 1)
- Interior surface of insulation (pos. 2)
- Interior surface (pos. 3)

Concerning the 2-dimensional simulation of the thermal bridges with WUFI® 2d, the positions described above are also evaluated at the standard cross section (results serving as a quality conformance check of 1d and 2d simulations), and additionally directly below the thermal bridge (i. e. the ceiling) (. Hence, the following positions will be evaluated:

- Rear of insulation (pos. 1 & 5)
- Interior surface of insulation (pos. 2 & 6)
- Interior surface (pos. 3 & 7)

Additionally, the wood moisture inside the wooden beam will be evaluated at critical positions. Hereby, sections of 10x10 mm at the lower side of the beam will be used:

- Beam head (pos. 4)
- Rear of insulation (pos. 5)
- Interior surface of insulation (pos. 6)

According to WTA guideline [5], the following assessment criteria will be used:

- Concerning frost risk:
30 % degree of saturation (relation of moisture content and maximum moisture); (a higher degree of saturation is acceptable when 95 % relative humidity (RH) within the construction are not outrun).
- Concerning biodegradation (wood decay):
20 M.-% wood moisture; ((slightly) higher maxima are acceptable for up to 6 month).
- Concerning mold growth:

80 % relative humidity.

If not specifically mentioned, all descriptions, results and values in this report refer to floating monthly average values.

2.2 Construction assembly & materials

According to the offer and specifications provided by the client, several constructions are employed in hygrothermal simulations. In the following, the general constructions and materials are stated. The assemblies are shown in figures 1 and 2, the basic material properties are stated in table 1.

For the one-dimensional simulation (figure 1), the basic construction of the wall is the following (listed from outside to inside):

- Lime-cement render, 20 mm
- Hollow concrete block, 200 mm
- Icynene foam, 180 mm
- Air layer, 50 mm
- Fermacell board, 10 mm

For the two-dimensional simulation (figure 2), one of the following materials/assemblies is inserted into the wall structure:

- Concrete ceiling, 250 mm
- Wooden joist, 250 mm & wooden floor, 20 mm

All material properties are measured values taken from the WUFI®-database.

2.3 Orientation, surface transfer & initial conditions

The hygrothermal impact on a façade differs depending on its orientation. Parameters like solar radiation or main driving rain direction usually play an important role. To do a holistic study of the worst case scenario of a interiorly insulated wall, it is necessary to determine the façade orientation exposed to the highest hygrothermal strain. This strain can be caused by low impact of radiation as this reduces the constructions drying potential – here, this would be northern orientation. Of importance in this respect is also the façade with highest impact of driving rain – southwestern orientation in this case. Therefore, in a first step, the wall assembly is simulated facing different directions (from north to south). In this way, a basis can be created for all further simulations that features the highest (worst case) hygrothermal conditions of the construction.

The surface transfer coefficient at the interior surface is $8 \text{ W}/(\text{m}^2\text{K})$. At the exterior side, the surface transfer is defined as wind dependent. The short wave radiation absorption factor is 0,2. The exterior surface features a comparatively

low water uptake (A-value) of $0,2 \text{ kg}/(\text{m}^2\cdot\text{h})$. The initial moisture content of all materials is 80 % RH; the initial temperature is $20,0 \text{ }^\circ\text{C}$.

2.4 Boundary conditions

The investigations are executed for the location of Nancy. Nancy is a city in the northeast of France; its conditions are held critical-representative for French climate. The annual mean temperature is $9,2 \text{ }^\circ\text{C}$, with minima and maxima ranging from $-13,5 \text{ }^\circ\text{C}$ to $32,3 \text{ }^\circ\text{C}$. The mean relative humidity is 78 % RH, with minima and maxima of 15 % RH and 100 % RH respectively. The mean wind velocity is $2,9 \text{ m/s}$, the normal rain amounts to 613 mm per year. The sum of counter radiation is $2782,1 \text{ kWh}/(\text{m}^2\text{a})$. Graphic images of temperature and relative humidity (hourly values and floating monthly average) are shown in figure 3.

The climate conditions at the interior side of the wall are applied according to the agreement with French DTU, as described in [6]. Hereby, the following conditions are set: Temperatures range in-between $20 \text{ }^\circ\text{C}$ (winter) and $25 \text{ }^\circ\text{C}$ (summer), according to the approach of EN 15026. Concerning RH, the French DTU conditions will serve as a basis, demanding a moisture level inside that is $5 \text{ g}/\text{m}^3$ higher than that of the outside; according to EN 13788, this approach is adapted slightly. Thus, with exterior temperatures below $0 \text{ }^\circ\text{C}$; the value of $5 \text{ g}/\text{m}^3$ stays remains unchanged; between $0 \text{ }^\circ\text{C}$ and $20 \text{ }^\circ\text{C}$, the value is reduced linearly to $0 \text{ g}/\text{m}^3$ and will stay at these conditions at higher temperatures, too. Graphics of temperature and relative are shown in figure 4.

3 Results

3.1 One-dimensional wall assembly

Figures 5 and 6 show the calculated hygrothermal conditions (total water content & relative humidity) of the construction for the different orientations according to one-dimensional simulation.

Starting from a construction moisture of 80 % RH, both total moisture content (MC) (figure 5) and relative humidity (RH) behind the insulation layer (pos. 1; figure 6) in all cases analyzed rise throughout the first heating period. In the first winter period, the highest total MC ($5,8 \text{ kg}/\text{m}^2$) is reached with western and northwestern orientation. The level of RH behind the insulation, however, shows that northern and northwestern orientation leads to highest maxima here. The higher MC of the western orientation in the first winter is due to the comparatively higher impact of driving rain here. In spring, conditions generally decrease again as the construction is drying out, showing minima in summer that undercut initial conditions. During the next years, dynamic equilibrium is reached. At this stage, northern orientation is showing highest maxima during winter both for total MC ($5,0 \text{ kg}/\text{m}^2$) as well as RH behind the insulation layer (92,9 % RH). During summer, too, highest values are shown by northern orientation, with a MC of $3,2 \text{ kg}/\text{m}^2$ and a RH of 71,0 % RH. Obviously, the low solar radiation at the northern façade plays a dominant role with respect to hy-

grothermal conditions in this case (conditions may change, however, with higher absorption of driving rain at the exterior surface). Northern direction will be used for all further simulations.

The results show that even for the worst-case orientation described above, conditions generally are unproblematic: At the rear side of insulation (pos. 1; figure 7, black curves) the boundary limit of 95 % RH is never exceeded even during winter time (max. 92,9 % RH); in summer, sufficient drying is shown (min. 71,0 % RH). Temperatures at this position never fall below the freezing point, reaching minima of 1,2 °C in winter and maxima of 21,8 °C in summer, hence, there is no frost risk here. Also, RH levels at this position are below limits according to WTA, hence, the degree of saturation must not be analyzed here. It is important, however, that a complete application of the foam is ensured to avoid convection behind the insulation layer.

Figure 8 (“standard cross section”) shows the levels of relative humidity and temperature at the interior surface of the insulation layer (pos. 2). Here, too, dynamic equilibrium is reached, with 59,1 % RH in winter and 48,6 % RH in summer. Temperatures show maxima of 24,3 °C and minima 18,6 °C. Due to effects of the insulation layer, the fluctuation range of both temperature and relative humidity is lower at this position compared to the rear side of insulation. At the interior surface (pos. 3; figure 9), conditions are even more favorable, with maxima of 60,0 % RH and 24,4 °C and minima of 47,6 % RH and 19,6 °C, thus, fluctuation range here is even lower than at the surface of insulation. At both positions, with RH levels below 80 % RH, mold growth conditions do not arise.

Within the context of Nancy climate conditions, hence, the standard cross section shows uncritical conditions altogether. Even if critical for French climate, the conditions in Nancy concerning driving rain and low winter temperatures remain on a level which doesn't require a vapor retarder for the investigated assembly.

3.2 Two-dimensional joints of wall and ceiling

3.2.1 Concrete ceiling

The blue curve in figure 7 shows the relative humidity at the rear side of insulation right below the concrete ceiling (pos. 5). Compared to the standard cross section, temperature decrease during winter is reduced due to the thermal bridge effect, illustrated also in figure 10, showing the temperature conditions on a cold winter evening (December 25th). The concrete ceiling possesses a comparatively high thermal conductivity, inducing an increased thermal flow from the interior towards the exterior. Hence, temperature minima behind the insulation in winter with 6,6 °C are approximately 5 °C higher at the thermal bridge than at the standard cross section. Due to the higher temperatures, RH maxima consequently are approximately 7 % RH lower, showing values of max. 76,1 % RH. The design criteria of 95 % RH thus are met.

More towards the interior, the thermal bridge has a contrary effect on the temperature conditions inside the wall: At the interior surface of the insulation layer (pos. 6), minima of 14,4 °C are shown right below the ceiling; thus, temperatures here are approximately 4 °C lower than at the standard cross section (figure 8). As can be seen in figure 10, the higher thermal conductivity of the concrete also leads to lower temperatures at the interior surface of insulation right below the concrete ceiling. As an effect of the lower temperatures, higher relative humidity levels arise during winter: With values of 67,6 % RH, maxima thus are approximately 8 % RH higher than at the standard cross section.

Similar are the results at the interior surface (pos. 7; figure 9). Here, too, the impact of the thermal bridge is noticeable. However, being in direct contact with the interior air, differences between thermal bridge and standard cross section are less distinct than e.g. at the interior of the insulation layer. Temperatures reach minima of 16,5 °C, approximately 3,1 °C lower than those at standard cross section. Relative humidity levels with maxima of 65,1 % RH are approximately 5 % higher.

Hence, moisture conditions at the thermal bridge are not critical altogether.

3.2.2 Wooden beam ceiling

Compared to the concrete ceiling, the thermal bridge effect of the wooden beam is less distinct, which can be seen in figure 11, showing the temperature conditions of the wooden beam/wall section on a cold winter evening (December 25th). This is mainly due to the greater conformity of the thermal conductivities of wood and insulation material. The wooden beam head (pos. 4), with maximum wood moisture content of 14,2 M.-% (figure 12), clearly stays below the wood decay limit of 20 M.-%. At the rear side of the insulation right below the beam (pos. 5; figure 7), temperatures are slightly higher than at standard cross section; consequently, maximum relative humidity (87,1 % RH during winter) is lower than at the standard cross section. Looking at the wood moisture content of the beam at the same position (figure 13) shows that only in the first year of calculation, limits are exceeded slightly (max. 20,8 M.-%). In the following years, however, moisture contents show a general decrease. At dynamic equilibrium, maximum moisture reaches 17,9 M.-%. Thus, design criteria are met. At the front of insulation (pos. 6) minimum temperatures of 17,1 °C and maximum RH levels of 60,8 % RH are shown (figure 8). Wood moisture conditions at this position (figure 14) also show comparatively low conditions with maxima of 10,5 M.-%. Here, too, design criteria are met. Conditions at the interior surface right below the wooden beam also are far below critical values: Minimum temperatures (18,9 °C) here are only slightly lower than at the standard cross section; thus, RH levels show uncritical maximum RH levels of 61,1 % RH. As these conditions are even less critical than those at the front of the insulation layer, wood moisture does not need to be analyzed, as it will not be problematic at these conditions, anyway.

Discussion & conclusions

The investigations show that at the comparatively moderate climate of Nancy (France) and with normal indoor climate conditions (for residential buildings), conditions inside the standard cross section stay below boundary values and thus are unproblematic. The two-dimensional simulation of the thermal bridges (joints wall/concrete ceiling & wall/wooden beam ceiling) also proves that no moisture related problems will occur. In none of the cases analyzed, critical conditions are present at dynamic equilibrium. Hence, the constructions can be done without an additional vapor retarder, if the assembly and conditions are similar to those analyzed in this study. Generally, it has to be assured that the exterior surface provides appropriate protection against driving rain, and that the installation of all layers at the interior side are executed in a high quality of workmanship, and do not bear any unintended air gaps and leakages.

5 Figures

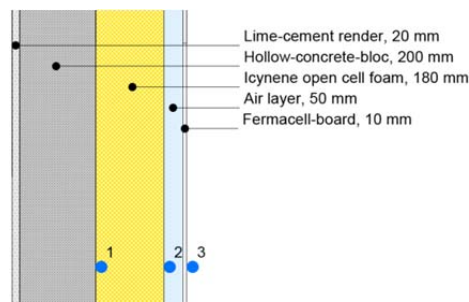


Figure 1:
Standard cross section of the interiorly insulated wall analyzed (WUFI® Pro) in this study.

Marked in blue are the monitor positions for the analysis of relative humidity:

- 1) Rear of insulation
- 2) Interior surface of insulation
- 3) Interior surface

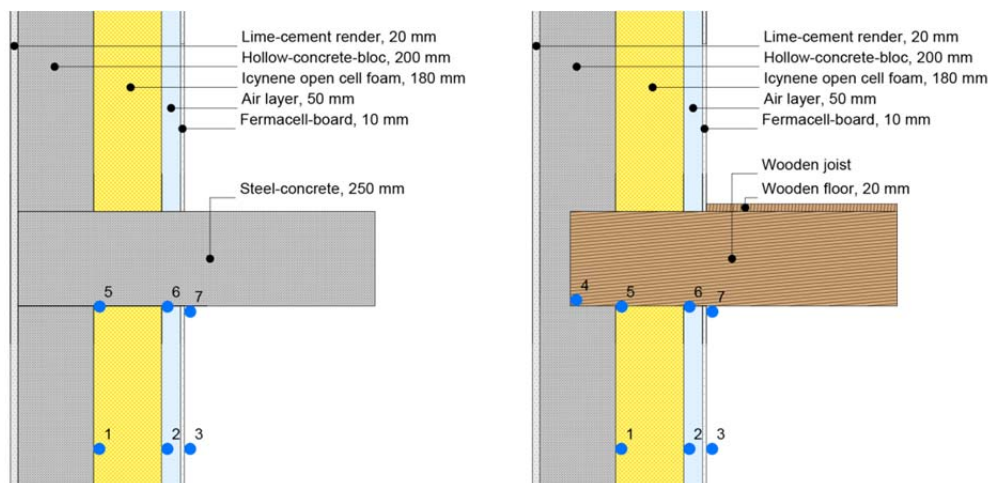


Figure 2:
Thermal bridges analyzed (WUFI® 2d) in this study.
Left: concrete ceiling; right: wooden beam ceiling.

Marked in blue are the monitor positions for the analysis of relative humidity (RH) and wood moisture (only wooden beam ceiling, analyzed is a wood section of approx. 10x10 mm).

- 1) Rear of insulation, standard cross section (RH)
- 2) Interior surface of insulation, standard cross section (RH)
- 3) Interior surface, standard cross section (RH)
- 4) Beam head, at lower exterior edge (wood moisture)
- 5) Rear of insulation, below/at thermal bridge (RH and wood moisture)
- 6) Interior surface of insulation, below/at thermal bridge (RH and wood moisture)
- 7) Interior surface, below thermal bridge (RH)

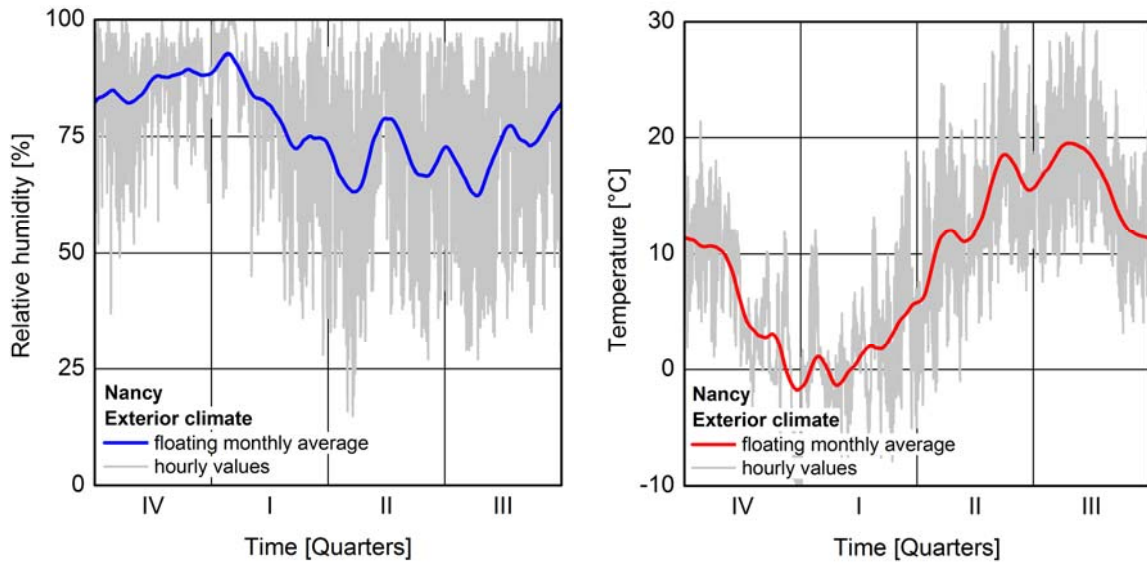


Figure 3:
Exterior climate conditions of Nancy (France) according to measurements. Left: relative humidity, right: temperature.

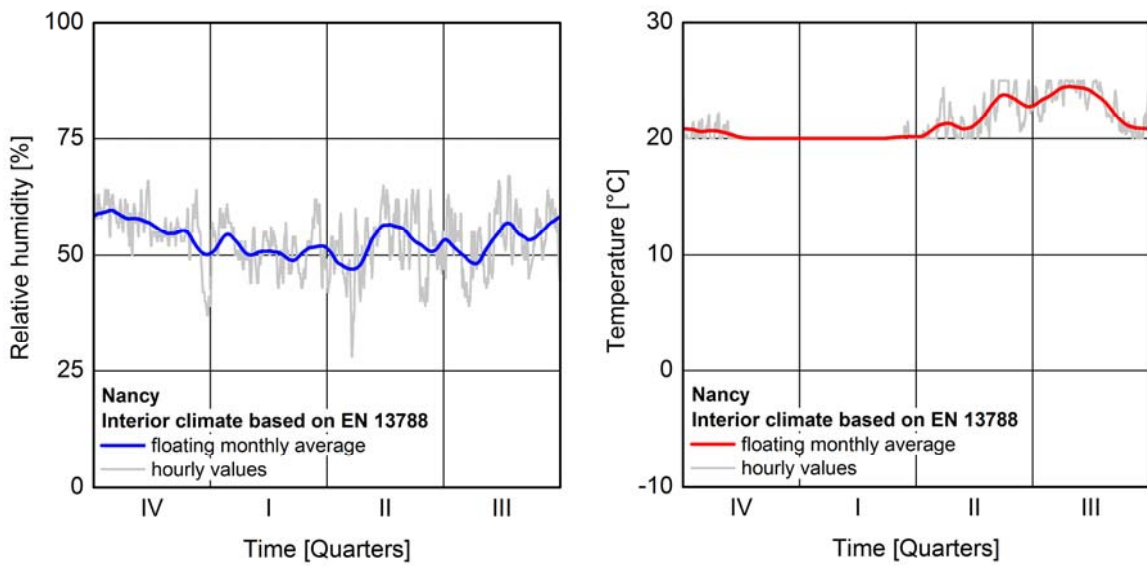


Figure 4:
Interior climate conditions of Nancy (France) based on EN 13788. Left: relative humidity, right: temperature.

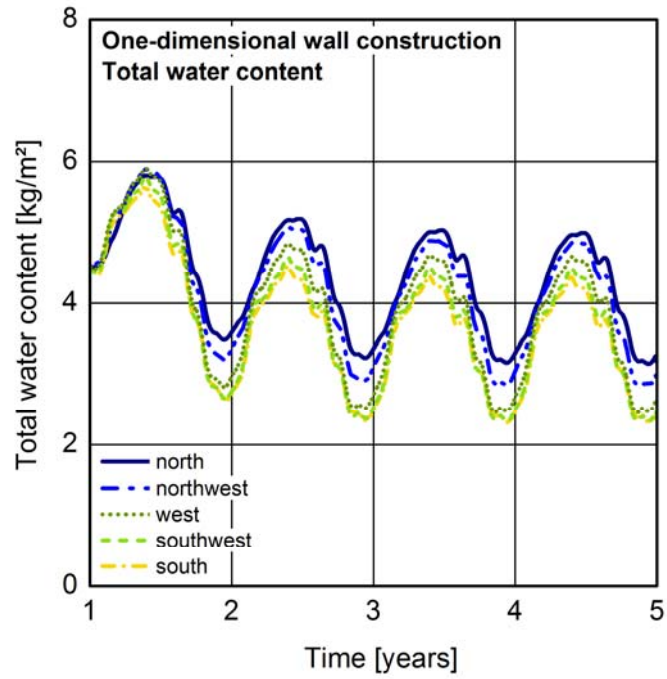


Figure 5: Analysis of the worst-case orientation in Nancy (France): Resulting water content (floating monthly average) of the construction.

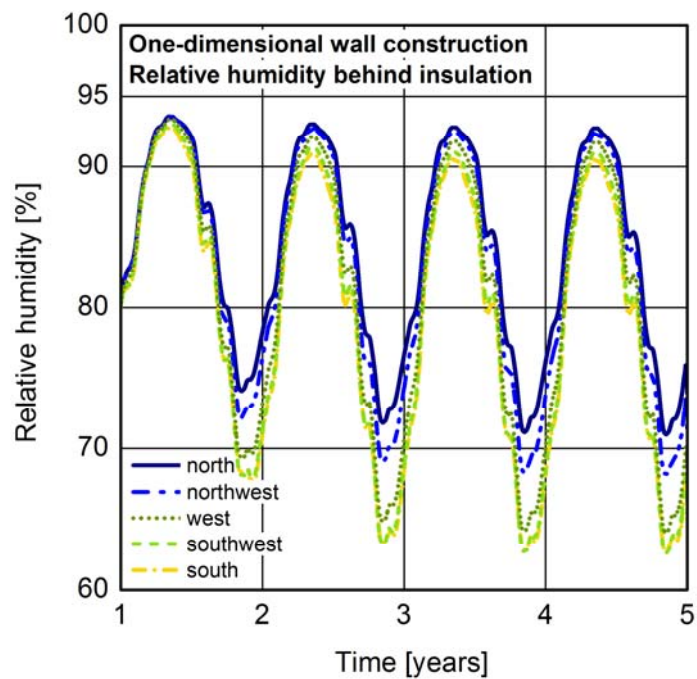


Figure 6: Analysis of the worst-case orientation in Nancy (France): Resulting relative humidity (floating monthly average) behind the insulation layer/at the interface of insulation and wall.

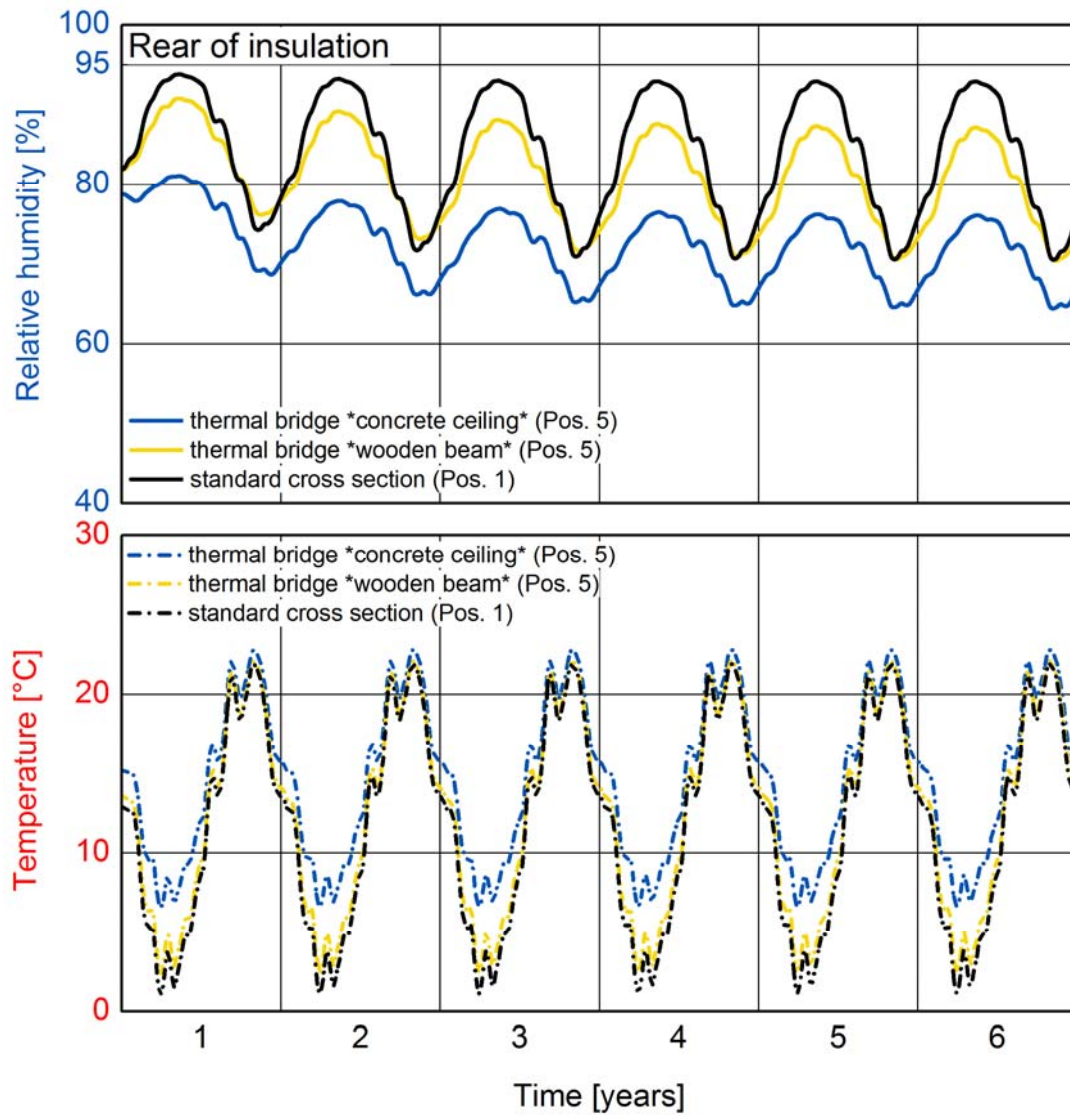


Figure 7:
 Temperature and relative humidity conditions behind the insulation layer at standard cross section and at the thermal bridge (below the ceiling/wooden beam).

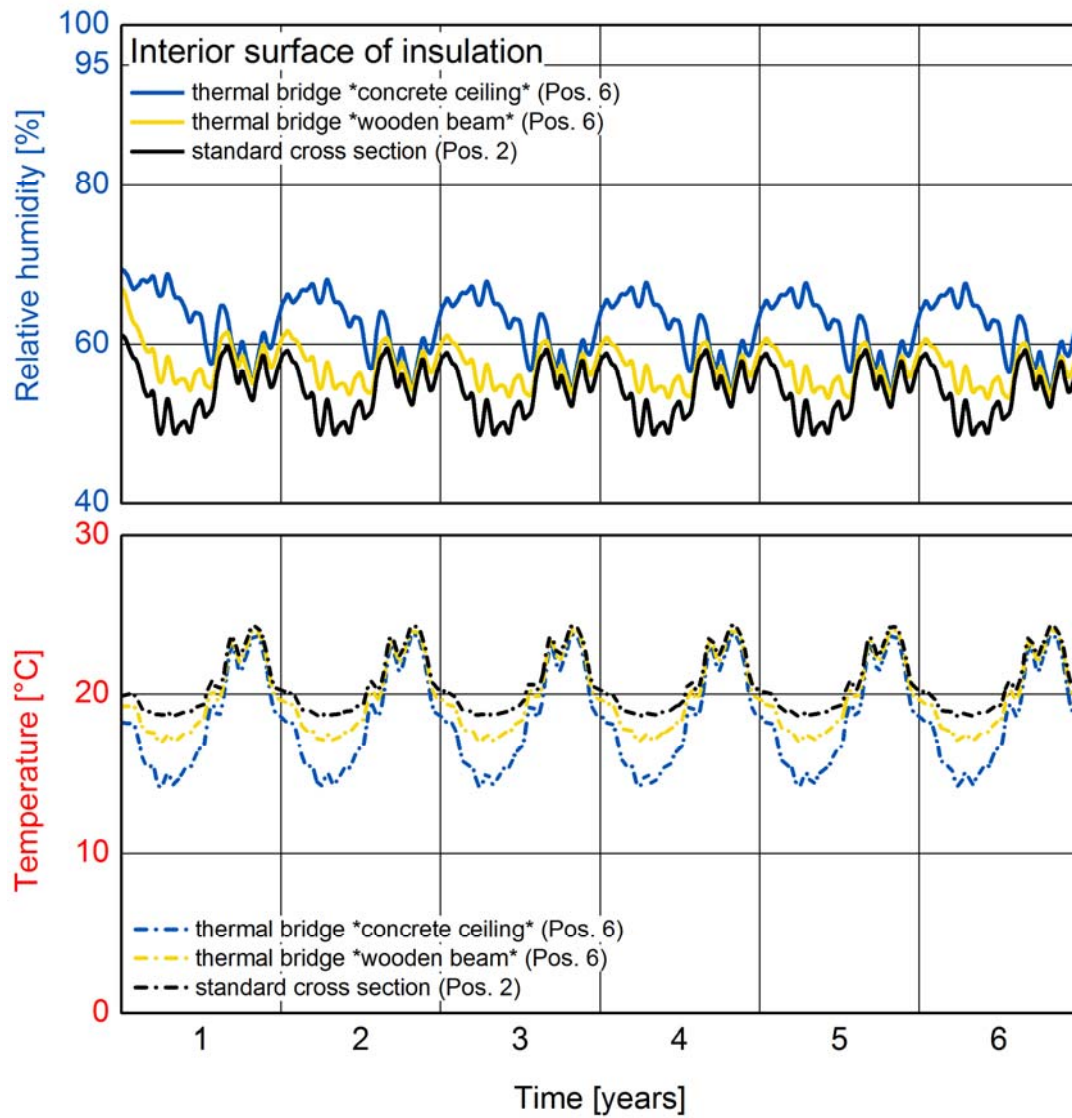


Figure 8: Temperature and relative humidity conditions at the front of the insulation layer at standard cross section and at the thermal bridge (below the ceiling/wooden beam).

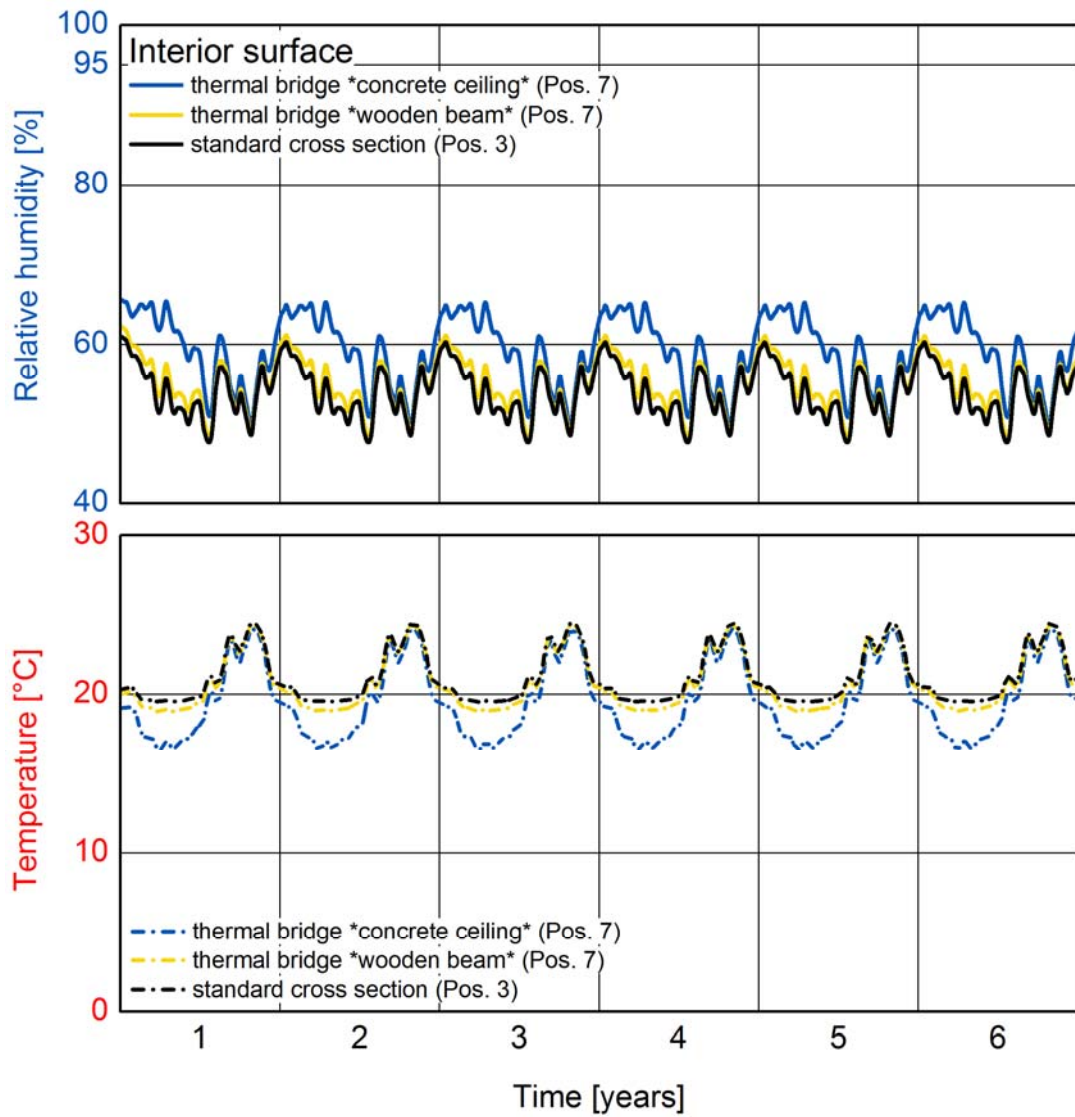


Figure 9:
 Temperature and relative humidity at the interior surface at the standard cross section and at the thermal bridge (below the ceiling/wooden beam).

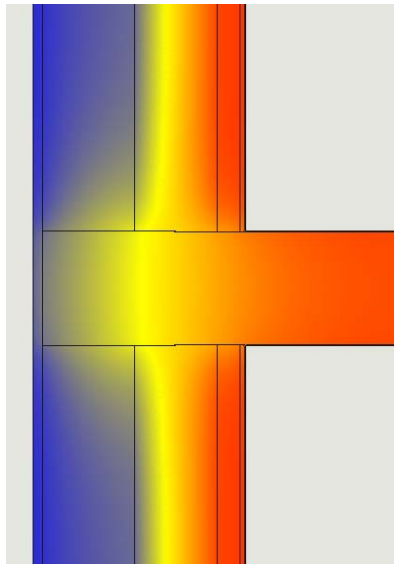


Figure 10:
Temperature conditions of the joint wall/concrete ceiling exemplarily for a cold winter evening (December 25th).

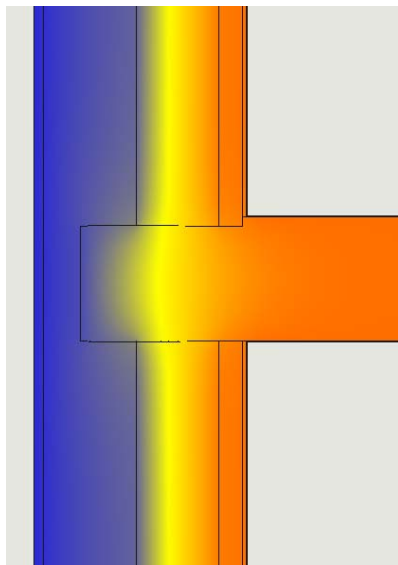


Figure 11:
Temperature conditions of the joint wall/wooden beam exemplarily for a cold winter evening (December 25th).

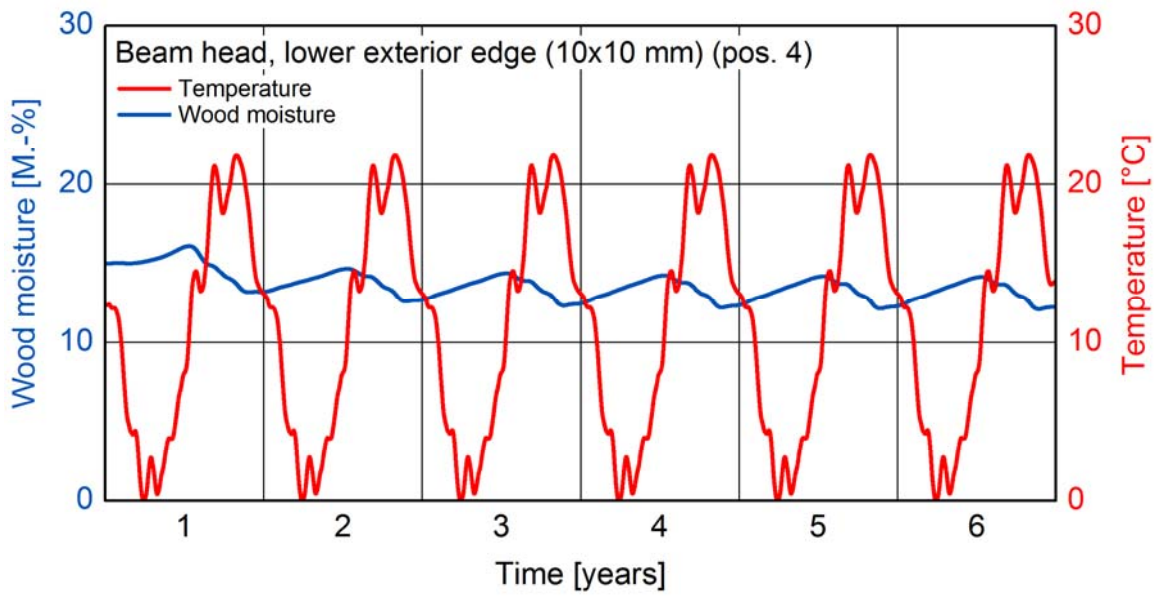


Figure 12:
Temperature and wood moisture conditions (floating monthly average) inside the wooden beam head, at its lower exterior edge.

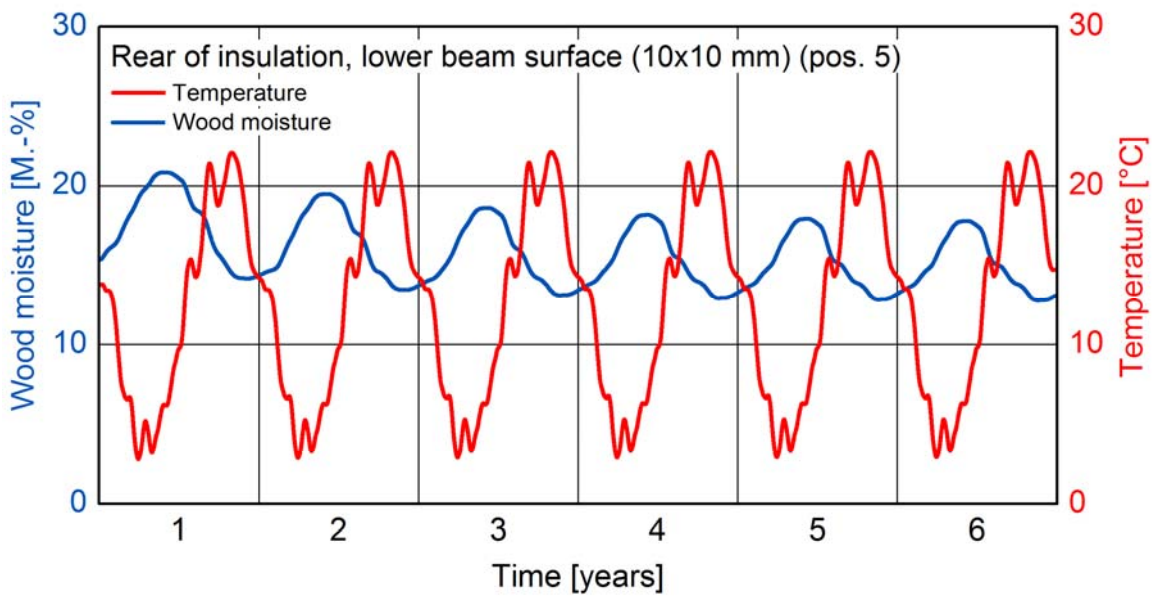


Figure 13:
Temperature and wood moisture conditions (floating monthly average) at the rear side of insulation inside the wooden beam.

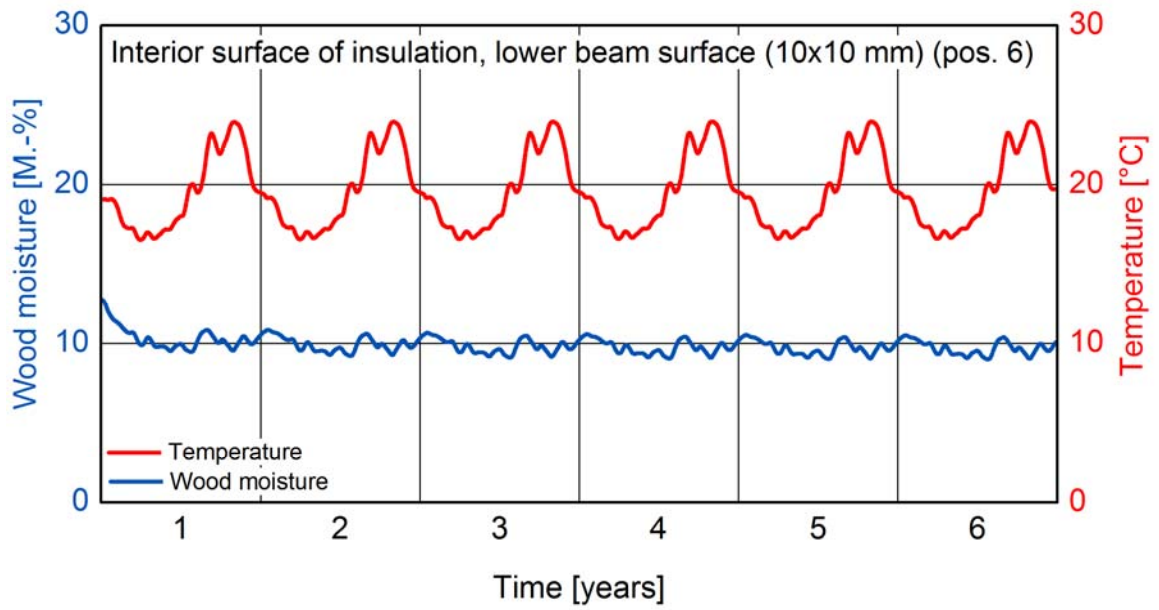


Figure 14:
Temperature and wood moisture conditions (floating monthly average) at the interior surface of insulation inside the wooden beam.

6 Tables

Table 1:
Material parameters of the interior insulation assemblies analyzed in this study.

Material	Density [kg/m³]	Porosity [%]	Thermal conduct. [W/(mK)]	Vapor resistance [-]
Lime-cement render (A-value= 0,2 kg/(m ² √h))	1900	24	0,8	20
Hollow concrete block	700	67	0,326	7,0
Icynene open cell foam	7,5	99	0,038	3,3
Fermacell board	1153	52	0,32	16
Concrete (ceiling)	2220	18	1,6	248
Softwood (beam)	400	73	0,09	200

Literature

- [1] Simultaneous Heat and Moisture Transport in Building Components. - One- and two-dimensional calculation using simple parameters. IRB Verlag (1995)
- [2] ASHRAE Standard 160P: Design Criteria for Moisture Control in Buildings. May 2009.
- [3] WTA-Merkblatt 6-1-01/D: Leitfaden für hygrothermische Simulationsberechnung.
- [4] WTA-Merkblatt 6-2-01/D: Simulation wärme- und feuchtetechnischer Prozesse. Mai 2002.
- [5] WTA-Merkblatt 6-5-12/D: Innendämmung nach WTA-II: Nachweis von Innendämmungen mittels numerischer Berechnungsverfahren. 2012.
- [6] Rapport „RAGE 2012 – Évaluation des risques de pathologies liées à l’humidité au niveau des poutres encastrées dans un mur extérieur isolé par l’intérieur“. Sept. 2013